Letter

Biocatalytic Access to Piperazines from Diamines and Dicarbonyls

Niels Borlinghaus, Sebastian Gergel, and Bettina M. Nestl

ACS Catal., **Just Accepted Manuscript** • DOI: 10.1021/acscatal.8b00291 • Publication Date (Web): 26 Mar 2018

Biocatalytic Access to Piperazines from Diamines and Dicarbonyls

Niels Borlinghaus, Sebastian Gergel and Bettina M. Nestl*

Institute of Biochemistry and Technical Biochemistry, Chair of Technical Biochemistry, Universitaet Stuttgart 70569 Stuttgart, Germany

ABSTRACT: Given the widespread importance of piperazines as building blocks for the production of pharmaceuticals, an efficient and selective synthesis is highly desirable. Here we show the direct synthesis of piperazines from 1,2-dicarbonyl and 1,2-diamine substrates using the *R*-selective imine reductase from *Myxococcus stipitatus* as biocatalyst. Various *N*- and *C*-substituted piperazines with high activity and excellent enantioselectivity were obtained under mild reaction conditions reaching up to 8.1 g per liter.

KEYWORDS: piperazines • double reductive amination • imine reductase • substrate scope • enantioselectivity • N- and C-substituted heterocycles

The piperazine moiety is a common structural motif in biological and pharmacological active compounds across a number of therapeutic areas.[1,2] Examples of piperazine containing pharmaceuticals include Imatinib, Palbociclib, Dasatinib, Sildenafil or Aripiprazole that reached a multi-billion revenue in 2016.[3] Selective methods for the formation of piperazines have been of long standing interest to the synthetic community. Classical methods for the selective preparation of substituted piperazines include the reduction of pyrazines or (di)ketopiperazines and metal-mediated or -catalyzed reductive cyclization reactions.[4–12] Here it should be noted that also *C*-substituted piperazines gain increasing importance for the design of promising drugs.[13–15] Prominent examples like Indinavir, used for HIV treatment, and Mirtazapin for treatment for depression are shown in Figure 1. Considering these progresses, efficient and facile methods for the synthesis of structurally diverse *C*-substituted piperazines that provide high regio-, stereo- and enantioselectivity are still in great demand.[5]

Despite the abundance of this heterocyclic motif in pharmaceutical compounds, natural piperazine containing alkaloids are relatively rare. Substitutions at 2' and 5' positions indicates that these alkaloids are formed via dimerization of aminoaldehydes as demonstrated for the biosynthesis of herquline A in *Penicillium herquei*.[16–19] However, due to the inflexible arrangement of substituents, such a route is not beneficial. This also applies to other biosynthetic routes where different diketopiperazines are formed via dimerization of amino acids.[20,21]

With this in mind, we applied imine reductases (IREDs), a novel class of NADPH-dependent biocatalysts for the asymmetric reduction of various cyclic imines, thus generating chiral secondary and tertiary amines.[22–27] Various nitrogen-heterocycles have been prepared applying IRED-catalyzed biotransformations in single-step and cascade reactions. Indeed, substituted pyrrolidines, piperidines and tetrahydroisoquinolines were generated.[28–32] Moreover, the panel of chiral amine products was significantly expanded using IREDs acting as 'reductive aminases' for the reductive amination of carbonyls.[33–38]

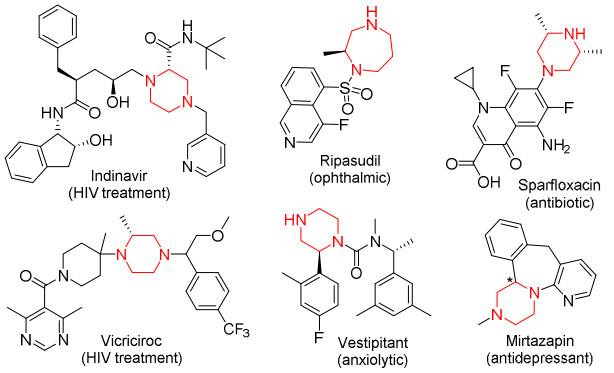

Figure 1. Representative pharmaceuticals containing chiral *C*-substituted piperazine building blocks and derivatives thereof. Piperazine and homopiperazine moieties are highlighted in red.

Intrigued by these results, we sought to further extend this catalyst system by generating piperazine derivatives directly from 1,2-diamines and 1,2-dicarbonyls in a double reductive amination reaction. Two C-N bonds have to be formed in this novel IRED-catalyzed approach to generate piperazine heterocycles. Most importantly, the use of appropriate substrates allows the introduction of substituents at each position of the piperazine moiety, which provides access to an invaluable scaffold in a modular fashion.

Taking into consideration that chiral amines were formed with high enantioselectivities in previously described

reductive aminations,[33] we began our studies by investigating enantiocomplementary imine reductases from *Streptosporangium roseum* (*R*-IRED_*Sr*) and from *Paenibacillus elgii* (*S*-IRED_*Pe*). In addition, we also tested the *R*-selective IRED from *Myxococcus stipitatus* (*R*-IRED_*Ms*), which has been the focus of recent attempts to induce the cofactor preference for NADH using enzyme engineering.[39] Reactions were monitored by measuring the depletion of the NADPH cofactor at 340 nm and detecting the generated products after performing biotransformations. The formation of piperazine (**1a**), 2-methyl piperazine (**2a**) and 1-methyl-3-phenyl piperazine (**3c**) was determined using a small representative library of 1,2-dicarbonyl and 1,2-diamine substrates (Table 1).

Table 1. Activity and selectivity in the double reductive amination using three enantiocomplementary IREDs[a].

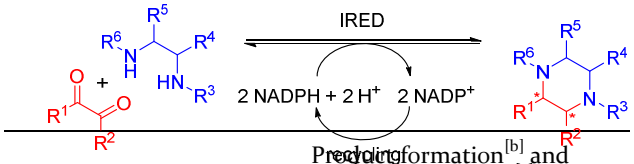

		Product formation[b] and enantiomeric excess[c] / %		
Entry	**Piperazine**	*R*-IRED_*Ms*	*R*-IRED_*Sr*	*S*-IRED_*Pe*
1	 **1a**	84 ± 5	14 ± 1	0
2	 **2a**	95 ± 7 > 99 (*R*)	> 99 94 (*R*)	33 ± 7 88 (*S*)
3	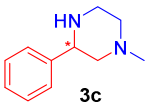 **3c**	> 99 > 99 (*R*)	7 ± 1 56 (*R*)	4 ± 1 17 (*S*)

[a] Reaction conditions: 5 mM diamine, 6.25 mM dicarbonyl (continuously added), 1 mg mL^{-1} IRED (purified protein), 2.5 mM NADPH, 40 mM glucose-6-phosphate, 5 U mL^{-1} glucose-6-phosphate dehydrogenase and 2.5 mM $MgCl_2$ in 50 mM potassium phosphate buffer pH 7.0, 25°C, 6 h. [b] Acetylated products were determined by GC. [c] Enantiomeric excess determined by chiral GC (entry 2) and HPLC (entry 3), respectively.

While moderate to high formation of **2a** was observed with *S*-IRED_*Pe* and *R*-IRED_*Sr* respectively, little amounts of product **3c** were formed with both enzymes. *R*-IRED_*Ms* showed best overall activity with up to >99% product formation (entries 1-3). We were delighted to observe that products **2a** and **3c** were obtained with excellent enantiomeric excess (>99% *ee*). Control experiments revealed that no piperazine formation was observed in the absence of IRED catalyst or NADPH.

In a recent study, it was shown that 1,2-diamines are not suitable amine donors for reductive aminations.[34] In this context, diamines and dicarbonyls were not used simultaneously in reductive amination reactions. This may reflect the fact that due to the high reactivity of diamine and dicarbonyl substrates, condensation products and oligomers can emerge spontaneously.[40] Moreover, different 1,2-dicarbonyls are known for their toxic effect on proteins by modifying arginine and other amino acids.[41] Strikingly, *R*-IRED_*Ms* is able to overcome these limitations and forms 69% of product **1a** in a batch biotransformation (data not shown) and 84% **1a**, when the dicarbonyl is fed continuously over 5 h.

From a mechanistic point of view, two general pathways can be proposed for the IRED-catalyzed synthesis of piperazines. Scheme 1 illustrates potential reaction routes in the formation of **1a** (for further details see also Supporting Information Figure S1).

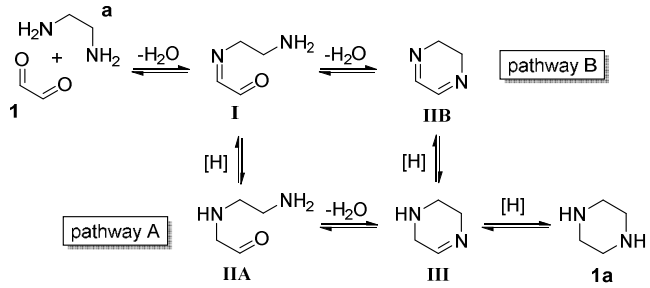

Scheme 1. Proposed reaction pathways A and B for the IRED-catalyzed synthesis of piperazine (1a).

The overall reaction consists of two condensation as well as two reduction steps. We propose that in pathway A the first condensation step is followed by a reduction and the formation of intermediate **IIA**. A further condensation step forms intermediate **III**, which is finally reduced to the piperazine product **1a**. In pathway B two consecutive condensation reactions take place to give the cyclic diimine intermediate (**IIB**). In subsequent reduction steps intermediate **III** and the corresponding piperazine product are formed.

It is known, that imine intermediates are unstable with respect to hydrolysis in aqueous media and thus, are in equilibrium with respective aldehydes. As a consequence, intermediates **IIA** and **IIB** can occur in both pathways. In this context, the detection of any intermediate does not indicate which pathway is preferred. However, we were able to synthesize 5,6-dimethyl-2,3-dihydropyrazine, which constitutes a diimine intermediate with enhanced hydrolysis stability (Figure S1). This compound also represents intermediate **IIB** in pathway B in the formation of **4a**. Interestingly no NADPH depletion and product formation was detected, using 5,6-dimethyl-2,3-dihydropyrazine as substrate, while product formation of **4a** was detected in biotransformations starting from the corresponding dicarbonyl (**4**) and diamine (**a**). This result demonstrates, that *R*-IRED_*Ms* prefers pathway A during

the formation of **4a**. We assume that this hypothesis can be also transferred to other substrate combinations.

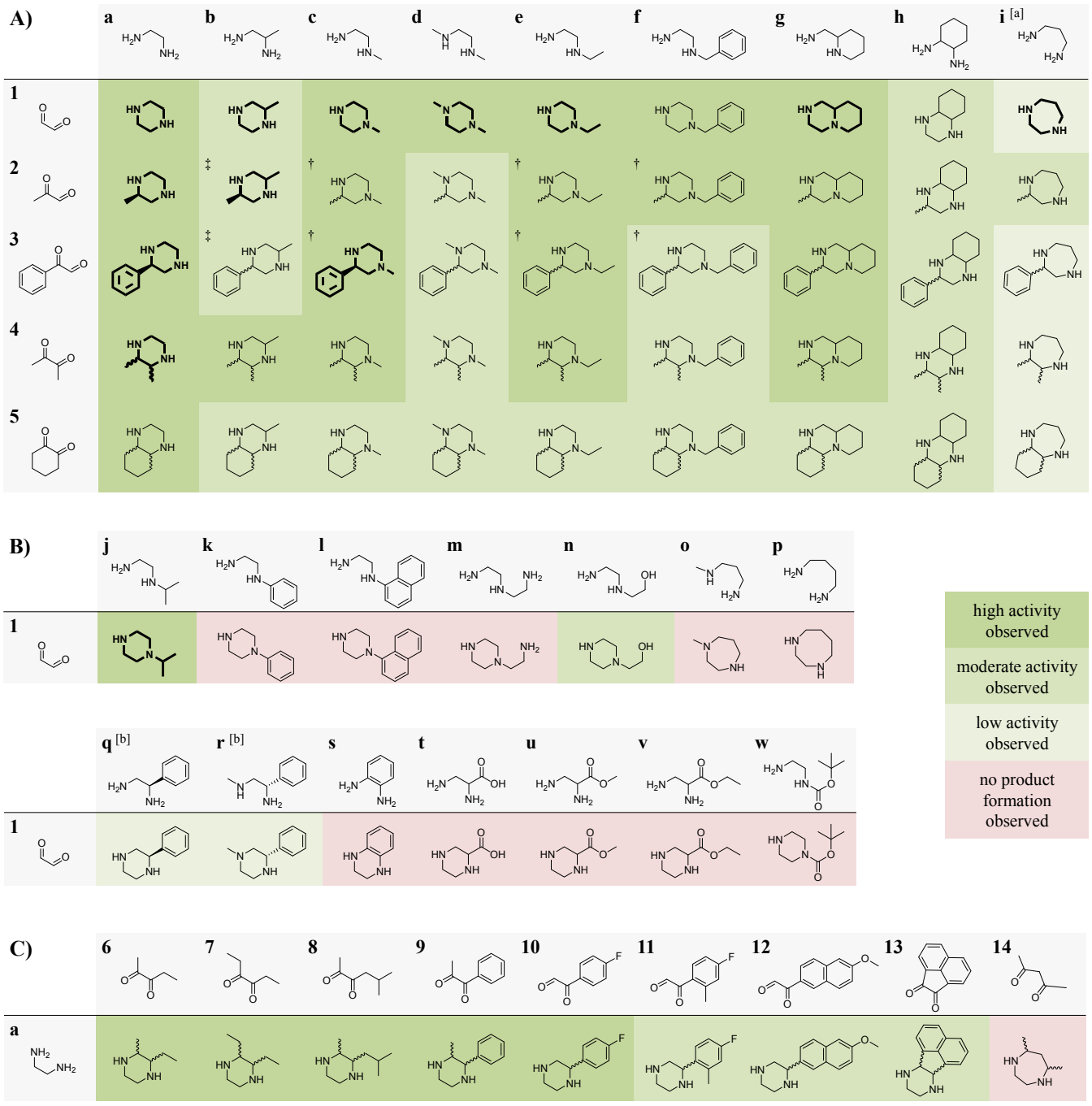

Figure 2. Scope of piperazines, homopiperazines, 1,4-diazocanes and derivatives thereof synthesized by *R*-IRED_*Ms* from a panel of dicarbonyl compounds and diamine reacting partners.

Five dicarbonyls were screened against nine diamines (**1a-5i**, Table section A). Double reductive aminations were further explored using glyoxal (**1**) as dicarbonyl with diamines **j-w** (Table section B), as well as ethylenediamine (**a**) with dicarbonyls **6-14** (Table section C). Structures of quantified products are highlighted in **bold** with values given in Table 2. The qualitative color coding is based on the photometrical determination of NADPH depletion and detection of product formation (see also Figure S3). Reaction conditions: 5 mM diamine, 5 mM dicarbonyl, 1 mg mL^{-1} purified *R*-IRED_*Ms*, 2.5 mM NADPH, 40 mM glucose-6-phosphate, 2.5 mM $MgCl_2$, 5 U mL-1 glucose-6-phosphate dehydrogenase in 50 mM potassium phosphate buffer pH 7.0, 25 °C, 4 h. Heterocycle formations were determined by GC-MS as acetylated molecules. [a] Enzyme concentration was increased to 2 mg mL^{-1} and 6.25 mM of dicarbonyl was fed continuously over 5 h. Reactions were stopped after 6 h. [b] Enzyme concentration was increased to 4 mg mL^{-1} and 6.25 mM of dicarbonyl was fed continuously over 5 h. Reactions were stopped after 6 h. [†] One of two possible regioisomers was detected. [‡] Both possible regioisomers were detected.

Table 2. Product formations, yields and selectivities in the synthesis of selected piperazines.

Piperazines	Product formation[a] / %	Product formation at higher concentration[c] / % (g L^{-1})	Isolated yield / % (mg)	Enantiomeric excess / %	Diastereomeric ratio	Regioisomeric ratio
1a	84 ± 5	10 ± 1 (0.4)	6 (0.5)	-	-	-
1b	39 ± 1	n.d.	n.d.	n.a.	-	-
1c	89 ± 5	n.d.	n.d.	-	-	-
1d	85 ± 3	n.d.	n.d.	-	-	-
1e	> 99	n.d.	n.d.	-	-	-
1g	> 95	n.d.	n.d.	n.a.	-	-
1i [b]	1.5 ± 0.1	n.d.	n.d.	-	-	-
1j	> 99	n.d.	n.d.	-	-	-
2a	> 95	68 ± 7 (3.4)	65 (6.0)	> 99 (*R*)	-	-
2b	40 ± 2 [d]	n.d.	n.d.	> 99 (*R*)	n.d.	2 : 1
3a	> 99	n.d.	n.d.	90 ± 1 (*R*)	-	-
3c	> 99 [d]	92 ± 9 (8.1)	87 (9.5)	> 99 (*R*)	-	> 99 : 1
4a	71 ± 2	n.d.	n.d.	n.d.	97 : 3 (*trans*)	-

[a] Reaction conditions: 5mM 1,2 diamine, 6.25 mM 1,2 dicarbonyl (continuously added), 1 mg mL^{-1} *R*-IRED_*Ms* (purified protein), 2.5 mM NADPH, 40 mM glucose-6-phosphate, 10 U mL^{-1} glucose-6-phosphate dehydrogenase, 2.5 mM $MgCl_2$ in 50 mM potassium phosphate buffer pH 7.0, 25°C, 6 h. Products were detected in their acetylated form via GC. [b] Due to low activity, the enzyme concentration was increased to 2 mg mL^{-1}. [c] Substrate concentrations were 10-fold increased to 50 mM (1,2-diamine) and 62.5 mM (1,2-dicarbonyl). Mass concentration was measured after 6 h. [d] Refers exclusively to the regioisomer depicted in Figure 2. n.a. not applicable (stereocenter is not generated by IRED). n.d. not determined.

In efforts to assess the scope of the piperazine forming double reductive amination and the substrate specificity of *R*-IRED_*Ms*, 68 different substrate combinations were examined by monitoring NADPH depletion (Figure 2). We thus investigated 23 diamines and 14 dicarbonyls to obtain a diverse set of piperazines with varying size and substitution patterns. For most reactions we observed a significant consumption of NADPH in the photometric assay. Additional biotransformations were performed in order to confirm the activity by detecting the formed products, which was successful for 57 different substrate combinations (highlighted in green, Figure 2). Product standards were commercially available for 13 substrate combinations that facilitated a more detailed and quantitative analysis (bold marked structures in Figure 2, values are given in Table 2). Remarkably, several alkyl and aryl groups were well accepted as *N*- and *C*-substituents and various bi- or tricyclic products were generated from monocyclic substrates. We were delighted to observe also the formation of homopiperazines (**1i**-**5i**) using 1,3-diaminopropane (**i**). No activity was observed when an aromatic system was directly linked to the amino group (**1k**, **1l**, **1s**, highlighted in red, Figure 2). Also no product formation was detected, when carboxy- or ester-functionalized diamines were used (**1t**-**1w**), which indicated that these additional functional groups hamper IRED activity. Interestingly, different *N*-alkyl substituents at the diamine substrate increased the activity (**1a** versus **1c**, **1e** and **1j**, Table 2). Notably, *C*-substitution at the diamine substrate decreased the activity, which is also indicated by low product formations of **1b**, **1q** and **1r**. It was noticed that this trend is inverted for the dicarbonyl substrates. Methyl- and phenylglyoxal were even better converted than the non-substituted glyoxal, for example **1a** versus **2a** and **3a** as well as **1c** versus **3c**.

In some cases, when we combined substituted diamines with substituted dicarbonyls, two possible regioisomers can be formed. However, only one regioisomer could be detected in the reaction of *N*-substituted diamines with *C*-substituted dicarbonyls (Figure S7). This is further illustrated by the synthesis of **3c**, where the phenyl group is only placed at the 3' position and not at the 2' position next to the *N*-methyl group. We assumed that for products **2c**, **2e**, **2f**, **3e** and **3f** also the 3' position is preferred due to steric advantages. In the reaction of *C*-substituted diamines with *C*-substituted dicarbonyls, no strict regioselectivity was observed and both regioisomers were detected (**2b**, **3b**, see Table S1). Furthermore we observed two diastereomers in varying ratios when disubstituted dicarbonyls (**4**-**9**) have been used (Figure S8). In this respect we assume a direct link to the tautomerization of intermediate **III** to the corresponding enamine, causing the racemization of one stereocenter (Figures S1 and S2). Consequently, high diastereomeric ratios could only be achieved when the final reduction step outcompetes the

tautomerization. The highest diastereomeric ratio (97:3) was found for product **4a**.

Finally, we tested the synthetic applicability of *R*-IRED_*Ms* in synthesizing piperazines using increased substrate concentrations (10-fold). Piperazines **2a** and **3c** comprise highly interesting building blocks in the synthesis of Vicriciroc and Mirtazapine. High production formations and yields of up to 92% and 87%, respectively, could be obtained with 10-fold higher substrate concentrations and 1 mg mL^{-1} *R*-IRED_*Ms*. Piperazines **2a** and **3c** were successfully formed, achieving 3.4 g L^{-1} and 8.1 g L^{-1} respectively in 6 h (Table 2). In summary, we have shown for the first time that IREDs can be used for the direct synthesis of piperazine heterocycles from readily available diamine and dicarbonyl starting materials. This way, a broad range of substituted piperazines becomes accessible in one step via double reductive amination. The demonstrated method also allows the synthesis of chiral piperazines tolerating aryl and alkyl substituted substrates and gives access to a novel and diverse set of piperazine building blocks with unique selectivity profiles. The advances shown here serve as the foundation for future progress in piperazine synthesis involving IREDs. The transformations should considerably facilitate the synthesis of an assortment of desirable molecules for research in chemistry, biology and medicine.

ASSOCIATED CONTENT

Supporting Information

General procedures, extended data about proposed mechanism, NADPH depletion assays, GC and HPLC analytics, chiral analysis and NMR data are included as Supporting Information. This material is available free of charge via the Internet at http://pubs.acs.org.

AUTHOR INFORMATION

Corresponding Author

* E-mail: bettina.nestl@itb.uni-stuttgart.de

ORCID ID

Bettina M. Nestl: 0000-0003-1282-195X

Notes

The authors declare no competing financial interest.

ACKNOWLEDGMENT

The research leading to these results received support from DFG (Deutsche Forschungsgesellschaft). We gratefully acknowledge the synthesis of *4*-fluorophenylglyoxal and *4*-fluoro-2-methylphenylglyoxal by Andreas Reichl.

REFERENCES

(1) Shaquiquzzaman, M.; Verma, G.; Marella, A.; Akhter, M.; Akhtar, W.; Khan, M. F.; Tasneem, S.; Alam, M. M. Piperazine scaffold: A remarkable tool in generation of diverse pharmacological agents. *Eur. J. Med. Chem.* **2015**, *102*, 487–529.

(2) Verma, S.; Kumar, S. Review Exploring Biological Potentials of Piperazines. *Med. Chem.* **2017**, *7*, 750–757.

(3) a) McGrath, N. A.; Brichacek, M.; Njardarson, J. T. A Graphical Journey of Innovative Organic Architectures That Have Improved Our Lives. *J. Chem. Educ.* **2010**, *87*, 1348–1349. b) Smith, D. T.; Delost, M. D.; Qureshi, H; Njarðarson, J. T. *Top 200 Pharmaceutical Products by Retail Sales in 2016 [online]*, available at: http://njardarson.lab.arizona.edu/sites/njardarson.lab.arizona.edu/files/2016Top200PharmaceuticalRetailSalesPosterLowResV3_0.pdf [Accessed 11 Jan. 2018].

(4) Gettys, K.; Ye, Z.; Dai, M.; Dong, H.-S.; Xie, Z.-X.; Luisi, R.; Reider, P. J. Recent Advances in Piperazine Synthesis. *Synthesis* **2017**, *49*, 2589–2604.

(5) Ye, Z.; Gettys, K. E.; Dai, M. Opportunities and challenges for direct C–H functionalization of piperazines. *Beilstein J. Org. Chem.* **2016**, *12*, 702–715.

(6) Rossen, K.; Weissman, S. A.; Sager, J.; Reamer, R. A.; Askin, D.; Volante, R. P.; Reider, P. J. Asymmetric hydrogenation of tetrahydropyrazines: Synthesis of (*S*)-piperazine-2-tert-butylcarboxamide, an intermediate in the preparation of the HIV protease inhibitor indinavir. *Tetrahedron Lett.* **1995**, *36*, 6419–6422.

(7) Huang, W.-X.; Liu, L.-J.; Wu, B.; Feng, G.-S.; Wang, B.; Zhou, Y.-G. Synthesis of Chiral Piperazines via Hydrogenation of Pyrazines Activated by Alkyl Halides. *Org. Lett.* **2016**, *18*, 3082–3085.

(8) Wang, Y.; Liu, Y.; Li, K.; Yang, G.; Zhang, W. Iridium-Catalyzed Asymmetric Hydrogenation of Unsaturated Piperazin-2-ones. *Adv. Synth. Catal.* **2017**, *359*, 1933–1941.

(9) Korch, K. M.; Eidamshaus, C.; Behenna, D. C.; Nam, S.; Horne, D.; Stoltz, B. M. Enantioselective Synthesis of α-Secondary and α-Tertiary Piperazin-2-ones and Piperazines by Catalytic Asymmetric Allylic Alkylation. *Angew. Chemie Int. Ed.* **2015**, *54*, 179–183.

(10) Nakhla, J. S., Wolfe, S. P. A Consice Asymmetric Synthesis of *cis*-2,6-Disubstituted N-Aryl Piperazines via Pd-Catalyzed Carboamination Reactions. *Org. Lett.* **2007**, *9*, 3279-3282.

(11) Nordstrøm, L. U.; Madsen, R. Iridium catalysed synthesis of piperazines from diols. *Chem. Commun.* **2007**, *0*, 5034-5036.

(12) Luescher, M. U.; Vo, C.-V. T.; Bode, J. W. SnAP Reagents for the Synthesis of Piperazines and Morpholines. *Org. Lett.* **2014**, *16*, 1236–1239.

(13) Ito, M.; Tanaka, T.; Cary, D. R.; Iwatani-Yoshihara, M.; Kamada, Y.; Kawamoto, T.; Aparicio, S.; Nakanishi, A.; Imaeda, Y. Discovery of Novel 1,4-Diacylpiperazines as Selective and Cell-Active eIF4A3 Inhibitors. *J. Med. Chem.* **2017**, *60*, 3335–3351.

(14) Kozlowski, J. A.; Zhou, G.; Tagat, J. R.; Lin, S.-I.; Mc Combie, S. W.; Ruperto, V. B.; Duffy, R. A.; Mc Quade, R. A.; Crosby Jr., G.; Taylor, L. A.; Billard, W.; Binch III, H.; Lachowicz, J. E. Substituted 2-(*R*)-methyl piperazines as muscarinic M(2) selective ligands. *Bioorg. Med. Chem. Lett.* **2002**, *12*, 791–794.

(15) Berger, R.; Zhu, C.; Hansen, A. R.; Harper, B.; Chen, Z.; Holt, T. G.; Hubert, J.; Lee, S. J.; Pan, J.; Qian, S.; Reitman, M. L.; Strack, A. M.; Weingarth, D. T.; Wolff, M.; MacNeil, D. J.; Weber, A. E.; Edmondson, S. D. 2-Substituted piperazine-derived imidazole carboxamides as potent and selective CCK1R agonists for the treatment of obesity. *Bioorg. Med. Chem. Lett.* **2008**, *18*, 4833–4837.

(16) Yu, X.; Liu, F.; Zou, Y.; Tang, M.-C.; Hang, L.; Houk, K. N.; Tang, Y. Biosynthesis of Strained Piperazine Alkaloids – Uncovering the Concise Pathway of Herquline A. *J. Am. Chem. Soc.* **2016**, *138*, 13529–13532.

(17) Kohmoto, S.; Kashman, Y.; McConnell, O. J.; Rinehart, K. L.;

Wright, A.; Koehn, F. Dragmacidin, a new cytotoxic bio(indole) alkaloid from a deep water marine sponge. *J. Org. Chem.* **1988**, *53*, 3116–3118.

(18) Enomoto, Y.; Shiomi, K.; Hayashi, M.; Masuma, R.; Kawakubo, T.; Tomosawa, K.; Iwai, Y.; Omura, S. Herquline B, a New Platelet Aggregation Inhibitor Produced by *Penicillium Herquei* Fg-372. *J. Antibiot.* **1996**, *49*, 50–53.

(19) Fujita, T.; Hayashi, H. New Brasiliamide Congeners, Brasiliamides C, D and E, from *Penicillium brasilianum* Batista JV-379. *Biosci. Biotechnol. Biochem.* **2004**, *68*, 820–826.

(20) Gu, B.; He, S.; Yan, X.; Zhang, L. Tentative biosynthetic pathways of some microbial diketopiperazines. *Appl. Microbiol. Biotechnol.* **2013**, *97*, 8439–8453.

(21) Mhaske, S. B.; Argade, N. P. The chemistry of recently isolated naturally occurring quinazolinone alkaloids. *Tetrahedron* **2006**, *62*, 9787–9826.

(22) Mitsukura, K.; Suzuki, M.; Tada, K.; Yoshida, T.; Nagasawa, T. Asymmetric synthesis of chiral cyclic amine from cyclic imine by bacterial whole-cell catalyst of enantioselective imine reductase. *Org. Biomol. Chem.* **2010**, *8*, 4533–4535.

(23) Mitsukura, K.; Suzuki, M.; Shinoda, S.; Kuramoto, T.; Yoshida, T.; Nagasawa, T. Purification and characterization of a novel (*R*)-imine reductase from *Streptomyces* sp. GF3587. *Biosci. Biotechnol. Biochem.* **2011**, *75*, 1778–1782.

(24) .Grogan, G.; Turner, N. J. InspIRED by Nature: NADPH-Dependent Imine Reductases (IREDs) as Catalysts for the Preparation of Chiral Amines. *Chem. - A Eur. J.* **2016**, *22*, 1900–1907.

(25) Mangas-Sanchez, J.; France, S. P.; Montgomery, S. L.; Aleku, G. A.; Man, H.; Sharma, M.; Ramsden, J. I.; Grogan, G.; Turner, N. J. Imine reductases (IREDs). *Curr. Opin. Chem. Biol.* **2017**, *37*, 19–25.

(26) Schrittwieser, J. H.; Velikogne, S.; Kroutil, W. Biocatalytic Imine Reduction and Reductive Amination of Ketones. *Adv. Synth. Catal.* **2015**, *357*, 1655–1685.

(27) Lenz, M.; Borlinghaus, N.; Weinmann, L.; Nestl, B. M. Recent advances in imine reductase-catalyzed reactions. *World J. Microbiol. Biotechnol.* **2017**, *33*, 199.

(28) Aleku, G. A.; Man, H.; France, S. P.; Leipold, F.; Hussain, S.; Toca-Gonzalez, L.; Marchington, R.; Hart, S.; Turkenburg, J. P.; Grogan, G.; Turner, N. J. Stereoselectivity and Structural Characterisation of an Imine Reductase (IRED) from *Amycolatopsis orientalis*. *ACS Catal.* **2016**, *6*, 3880–3889.

(29) France, S. P.; Hussain, S.; Hill, A. M.; Hepworth, L. J.; Howard, R. M.; Mulholland, K. R.; Flitsch, S. L.; Turner, N. J. One-Pot Cascade Synthesis of Mono- and Disubstituted Piperidines and Pyrrolidines using Carboxylic Acid Reductase (CAR), ω-Transaminase (ω-TA), and Imine Reductase (IRED) Biocatalysts. *ACS Catal.* **2016**, *6*, 3753–3759.

(30) Li, H.; Tian, P.; Xu, J.-H.; Zheng, G.-W. Identification of an Imine Reductase for Asymmetric Reduction of Bulky Dihydroisoquinolines. *Org. Lett.* **2017**, *19*, 3151–3154.

(31) Scheller, P. N.; Nestl, B. M. The biochemical characterization of three imine-reducing enzymes from *Streptosporangium roseum* DSM43021, *Streptomyces turgidiscabies* and *Paenibacillus elgii*. *Appl. Microbiol. Biotechnol.* **2016**, *100*, 1–12.

(32) Wetzl, D.; Berrera, M.; Sandon, N.; Fishlock, D.; Ebeling, M.; Müller, M.; Hanlon, S.; Wirz, B.; Iding, H. Expanding the Imine Reductase Toolbox by Exploring the Bacterial Protein-Sequence Space. *ChemBioChem* **2015**, *16*, 1749–1756.

(33) Scheller, P. N.; Lenz, M.; Hammer, S. C.; Hauer, B.; Nestl, B. M. Imine Reductase-Catalyzed Intermolecular Reductive Amination of Aldehydes and Ketones. *ChemCatChem* **2015**, *7*, 3239–3242.

(34) Aleku, G. A.; France, S. P.; Man, H.; Mangas-Sanchez, J.; Montgomery, S. L.; Sharma, M.; Leipold, F.; Hussain, S.; Grogan, G.; Turner, N. J. A reductive aminase from Aspergillus oryzae. *Nat. Chem.* **2017**, *9*, 961–969.

(35) Roiban, G.-D., Kern, M., Liu, Z., Hyslop, J., Tey, P. L., Levine, M. S., Jordan, L. S., Brown, K. K., Hadi, T., Ihnken, L. A. F., Brown, M. J. B. Efficient Biocatalytic Reductive Aminations by Extending the Imine Reductase Toolbox. *ChemCatChem* **2017**, *9*, 4475-4479.

(36) Matzel, P.; Gand, M.; Höhne, M. One-step asymmetric synthesis of (*R*)- and (*S*)-rasagiline by reductive amination applying imine reductases. *Green Chem.* **2017**, *43*, 788–824.

(37) Matzel, P.; Krautschick, L.; Höhne, M. Photometric Characterization of the Reductive Amination Scope of the Imine Reductases from *Streptomyces tsukubaensis* and *Streptomyces ipomoeae*. *ChemBioChem* **2017**, *18*, 2022–2027.

(38) Huber, T.; Schneider, L.; Präg, A.; Gerhardt, S.; Einsle, O.; Müller, M. Direct reductive amination of ketones: Structure and Activity of *S*-Selective Imine Reductases from *Streptomyces*. *ChemCatChem* **2014**, *6*, 2248–2252.

(39) Borlinghaus, N.; Nestl, B. M. Switching the Cofactor Specificity of an Imine Reductase. *ChemCatChem* **2018**, *10*, 183-187.

(40) Edwards, J. M.; Weiss, U.; Gilardi, R. D.; Karle, I. L. Formation of a heterocyclic cage compound from ethylenediamine and glyoxal. *Chem. Commun.* **1968**, *0*, 1649–1650.

(41) Takahashi, K. The Reactions of Phenylglyoxal and Related Reagents with Amino Acids. *J. Biochem.* **1977**, *81*, 395–402.

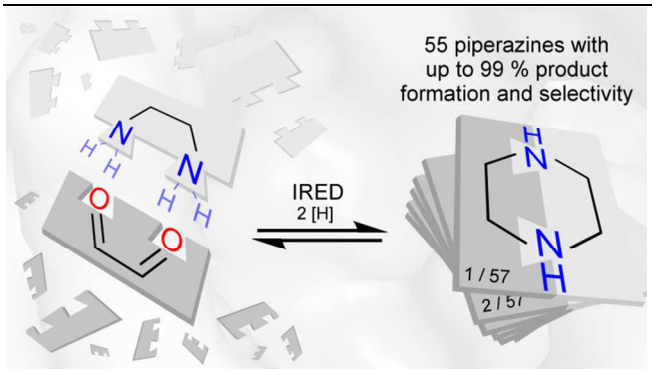
55 piperazines with
up to 99 % product
formation and selectivity
IRED
2 [H]
1 / 57

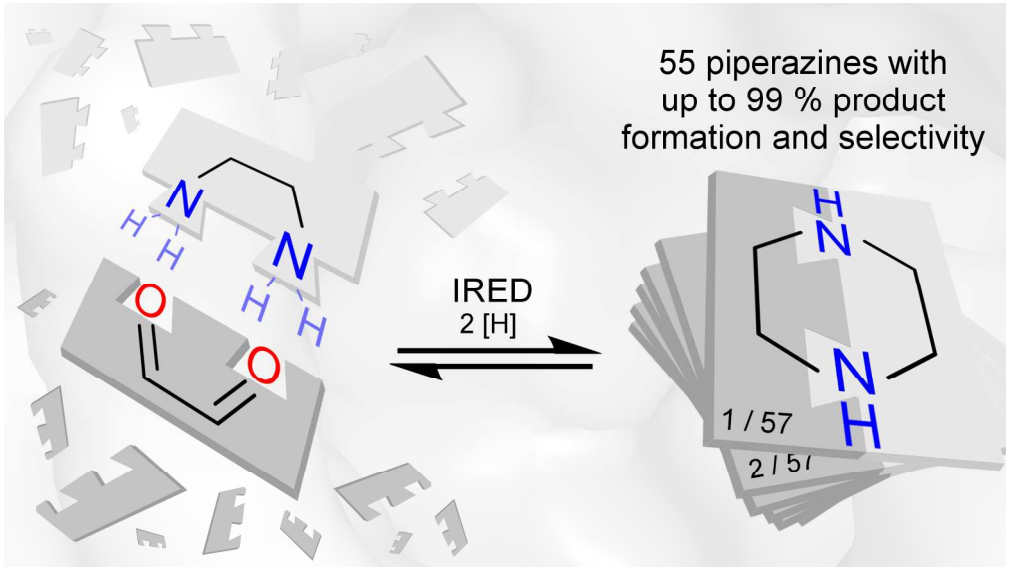

TOC graphic revised

845x476mm (72 x 72 DPI)

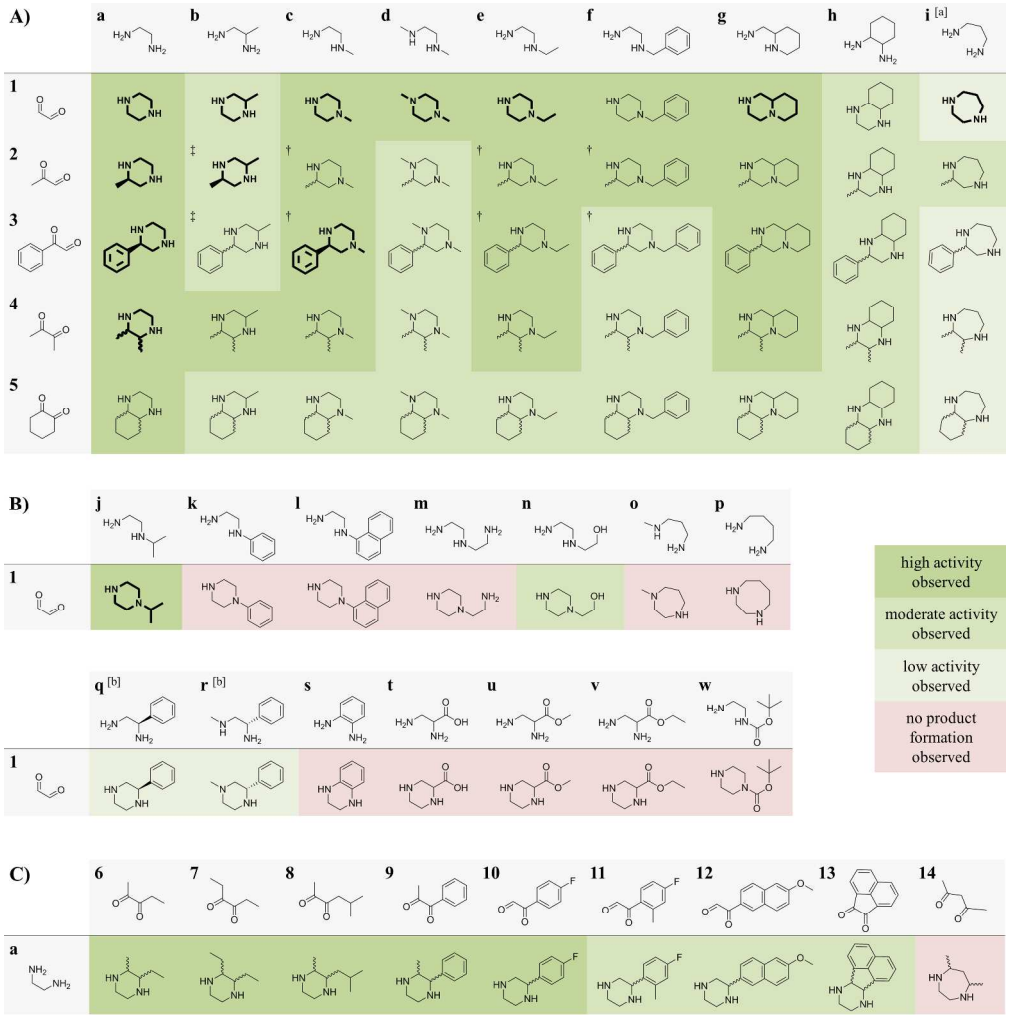

matrix template figure 2 revised

964x975mm (80 x 80 DPI)